Monolayer Characteristics of Mixed Octadecylamine and Stearic Acid at the Air/Water Interface

Yuh-Lang Lee,* Yaw-Chia Yang, and Yu-Jen Shen

Department of Chemical Engineering, National Cheng Kung University, Tainan 70101, Taiwan, ROC

Received: October 18, 2004; In Final Form: January 21, 2005

Mixed monolayers of stearic acid (SA) and octadecylamine (ODA) at the air/water interface were investigated in this article. The miscibility of the two compounds was evaluated by the measurement of surface pressure−area per molecule ($\pi-A$) isothems and the direct observation of Brewster angle microscopy (BAM) on the water surface. The two compounds were spread individually on the subphase (method 1) or premixed first in the spreading solvent and then cospread (method 2). The effect of spreading method on the miscibility of the two compounds was also studied. The results show that the mixed monolayers prepared by method 1 cannot get a well-mixed state. The isotherms of mixed monolayers preserve both characteristics of SA and ODA and exhibit two collapse points. The calculated excess surface area is very small. Besides, distinguished domains corresponding to those of pure SA and ODA can be inspected from the BAM images. Such results indicate that SA and ODA cannot get a well-mixed phase via 2-dimensional mixing. On the contrary, in the mixed monolyer prepared by cospreading, the two compounds exhibit high miscibility. In the $\pi-A$ isotherms, the individual characteristics of SA and ODA disappear. The calculated excess area exhibits a highly positive deviation which indicates the existence of special interaction between the two compounds. The low compressibility of isotherm implies the highly rigid characteristic of the mixed monolayer. which was also sustained by the striplike collapse morphology observed from the BAM. The rigid characteristic of SA/ODA mixed monolayer was attributed to the formation of "catanionic surfactant" by electrostatic adsorption of headgroups of SA and ODA or to the formation of salt by acid−base reaction.

Introduction

Langmuir−Blodgett (LB) deposition is a potential technique in fabrication nanothin film of controlled structure.[1−3] The Langmuir monolayer at the air/liquid interface plays an important role in the application of the LB technique.[4−6] For a traditional LB film of amphiphilic molecule, the film quality is intimately determined by the characteristics of the precursor monolayer. As an alternative method, Langmuir monolayer has been used as a template to adsorb nanoparticles (or their precursor compounds) for the assembly of particulate thin film.[7−9]

The behaviors of monolayers of fatty acids and their related LB films may be the most extensively studied systems for both research and application.[10−13] However, there has been little attention paid to the systematic study of fatty amine compared to that of fatty acids.[14−17] Because of to the contrary behavior to that of fatty acid, fatty amine offers a good substitution to solve the problem that cannot be overcome by fatty acid. For example, to prepare particulate thin film by adsorption of negatively charged particles into the monolayer template, fatty amine should be used due to its positive ionized state.[18,19] Langmuir monolayers of amine have also been used to deposit complex ammonium salts of organic or inorganic anions from an aqueous subphase for preparing ultrathin films of oxides or nanocluster of novel metal.[20,21] To be used as an adsorption layer, the subphase should be controlled at low pH where the amine molecules preserve an ionized state, Unfortunately, the amine monolayer is unstable on aqueous subphase of low bulk pH adjusted by hydrochloric acid. Various methods have been employed to improve the stability of amine monolayer either by using other acids such as $HClO_4$ or H_2SO_4 or by using mixed monolayer.[9,15]

Recently mixed monolayers have brought more and more interest in the monolayer research due to the vast properties of a multicomponents system than that of pure ones.[16,22−24] For some cases, monolayer of one component is not able to obtain good transfer ratio when deposition onto a solid substrate, and thus, the second component should be incorporated into the monolayer to promote the transfer.[25−27] For a mixed monolayer, the miscibility of various compounds is important to the stability and the later application of the LB deposition.

Because of the intensive studies of fatty acid and fatty amine monolayers, and their widely applications in the fabrication of nanoparticulate thin film,[7] SA and ODA are used as a model system to study the miscibility of the two components at the air/liquid interface and the behavior of their mixed monolayers. The relaxation behavior of SA/ODA mixed monolayer has been studied in a previous paper by spreading the two compounds individually onto the subphase.[28] The results show that the two components seem not completely miscible to be a homogeneous phase. In the present work, the miscibility of SA and ODA were intensively studied. Two spreading methods were used to study their effects on the 2-dimensional (2D) mixing of the two compounds. The characteristics of the mixed monolayers were evaluated by surface pressure (π)−mean molecular area (A) isotherms, excess area, and observation directly with Brewster angle microscopy (BAM).

* Corresponding author: e-mail yllee@mail.ncku.edu.tw; Fax 886-6-2344496.

10.1021/jp045251z CCC: $30.25
Published on Web 02/18/2005

Experimental Section

Materials. Octadecylamine (ODA, >99% pure) and stearic acid (SA, >99% pure) were purchased from Aldrich and Fluka, respectively. Both chemicals were used as received. Chloroform (>99% pure) was supplied by J.T. Baker and was used as the spreading solvent for the monolayer-formation materials. The concentrations of ODA and SA stock solutions were both 1 mg/mL. Pure water was used as subphase. The water used was purified by means of a Milli-Q plus water purification system with an electric resistance of 18.2 MΩ.

Method. The monolayer experiments and the LB films deposition were performed on a computer-controlled film-balance apparatus, KSV minitrough, constructed by KSV Instruments Ltd., Finland. The Teflon trough has a working area of 32 × 7.5 cm^2 and was placed on a vibration isolation table and closed in an environmental chamber. The film pressure at the air/water interface was measured by using the Wilhelmy plate arrangement attached to a microbalance. Pure water was used as subphase which has a measured pH value of 5.8 at the experimental temperature 25 °C. The sample containing monolayer-forming materials was spread on the subphase by microsyringe. Two different spreading methods are used to prepare the ODA/SA mixed monolayer. For the first one, appropriate quantities of ODA and SA stock solutions were individually added onto the subphase in sequence to control the monolayer composition. For the second method, SA and ODA were premixed in chloroform and then cospread onto the subphase. After allowed 20 min for solvent evaporation, the monolayer at the air/water interface was compressed at a rate of 2 $Å^2$/(molecule min). A surface pressure−area per molecule ($\pi-A$) isotherm was obtained by continuous compression of the monolayer by two moving barriers.

To observe the morphological characteristics of the monolayer at the gas/water interface by Brewster angle microscopy (BAM), a larger trough constructed by Nima Technlogy Ltd., England (model 601 BAM), was used. The trough has a working area of 70 × 7 cm^2, which is large enough to mount the BAM directly on it. The BAM used was designed by Nanofilm Technology (NFT), Göttingen, Germany (model BAM2 plus). The p-polarized light from an Nd:YAG laser, with a wavelength of 532 nm, was incident at Brewster angle (53.1°) to the air/water interface. Under such condition, the reflectivity of the beam was almost zero on the clean water surface. When an insoluble monolayer was present at the air/water interface, the beam reflects and an image was shown according to the organization of the monolayer. The images were visualized on a CCD camera and were recorded by means of a video recorder. The lateral resolution of BAM was about 2 μm. The BAM images were obtained during the compression process and recorded along the isotherm.

Results and Discussion

1. Monolayers Prepared by Spreading SA and ODA Individually. Isotherm Characteristics of Mixed Monolayers on Water Subphase. The surface pressure−area per molecule ($\pi-A$) isotherms for mixed ODA/SA monolayers at various compositions are demonstrated in Figure 1. Curves 1 and 7 were the isotherms for monolayers of pure SA and ODA, respectively. The lift-off value of the isotherm is 25 $Å^2$/molecule for SA and 17 $Å^2$/molecule for ODA. These values, as well as the shape of the isotherms, are consistent with those values reported in the literature,[14,29] and the smaller value of ODA was attributed to its higher solubility in water.[15] The isotherms for the mixed monolayers located between those of the pure chemicals and the lift-off area decrease with increasing ODA ratio in the mixed monolyers. A phase transition point was shown at $\pi \approx 27$ mN/m for SA monolayer and $\pi \approx 10$ mN/m for ODA. The phase transition point of SA monolayer can also be found in the isotherms of SA richer mixed monolayer but was eliminated when over 50 mol % of ODA was added. On the contrary, for the ODA richer mixed monolayers, a phase transition point corresponding to that of ODA monolayer was exhibited.

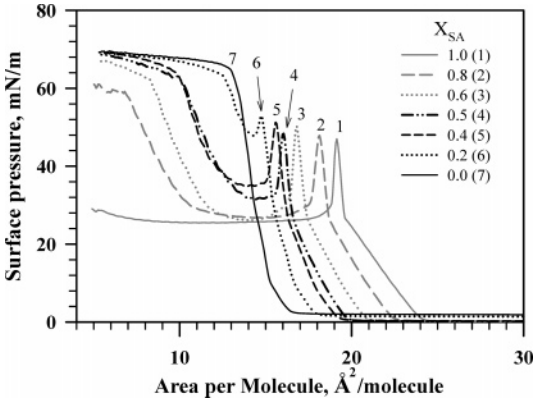

Figure 1. Surface pressure−area per molecule isotherms of mixed ODA/SA monolayers of various compositions.

The collapse surface pressures (π_c) of the monolayers were list in Table 1. The values of collapse pressures were 47 and 65 mN/m, respectively, for SA and ODA monolayers, and the values increase steadily with increasing ODA ratio in the mixed monolayers. According to the phase rule,[30] the two components in the mixed monolayers are miscible at the interface because the collapse surface pressure varies with composition. However, the appearance of the phase transition points similar to that of the pure compounds in the mixed monolayers also suggests the existence of the pure SA (or ODA) phase in the mixed monolayer. That is, the two components in the mixed monolayers are not completely miscible at the gas/liquid interface.

One interesting behavior which can be inspected from the isotherms of the mixed monolayers is the variation of surface pressure when the monolayer was further compressed after the collapse point. For SA monolayer, the surface pressure decreases abruptly after passing the collapse pressure and approaches a much lower constant value. However, the surface pressure of ODA monolayer does not decrease but, on the contrary, increases slightly after collapse. The surface pressure of mixed monolayer also decreases steeply after the first collapse point but increases further when the isotherm go through a valley. With increasing ODA ratio in the mixed monolayers, the surface pressure increases earlier after the first collapse point. The reincreased surface pressure can approach a value equivalent to the collapse pressure of an ODA monolayer. Such phenomena suggest that the mixed monolayers also process the individual characteristics of SA and ODA. It is likely that the first collapse point is caused from the collapse of SA domains in the mixed monolayer and the presence of ODA did increase this collapse pressure. The reincrease of surface pressure in the later compression stage indicates that there are domains that did not collapse in the first collapse point, and its constituent is supposed to be ODA.

The miscibility of a mixed monolayer can be examined by quantitative analysis of the excess area (A_{ex}) of the mixed monolayer at the air/water interface. The excess area can be obtained by comparing the average area per molecule of a mixed

TABLE 1: Collapse Surface Pressure (π_c) of SA/ODA Mixed Monolayer Prepared by Different Spreading Method

SA/ODA ratio	1/0	8/2	6/4	5/5	4/6	2/8	0/1
π_c estiamated by spread individually (mN/m)	47.0	47.2	49.0	47.5	50.0	53.0	65.0
π_c estiamted by spread after premixing (mN/m)	47.0	62.0	65.0	65.0	65.0	65.0	65.0

monolayer consisting of components 1 and 2 (A_{12}) with that of an ideal mixed monolayer (A_{id}).

$$A_{ex} = A_{12} - A_{id} = A_{12} - (X_1A_1 + X_2A_2) \quad (1)$$

where X_1 and X_2 are the mole fractions of components 1 and 2, respectively, in the mixed monolayer and A_1 and A_2 are the area per molecule of the pure monolayers at the same surface pressure.

For an ideal mixed monolayer or when the components in the mixed monolayer are immiscible, the excess area will be zero and A_{12} will be linear in X_1. Figure 2a illustrates the mean area per molecule as a function of composition of SA/ODA mixed monolayers at different surface pressure. Although the linearity between the mean molecular area and SA composition was not exactly observed, the deviation is only slight. The values of A_{ex}/A_{id} estimated from Figure 2a are shown in Figure 2b. In general, the mixed monolayers exhibit a negative deviation although few exceptions were also observed. The most significantly negative deviation appeared at $X_{SA} = 0.5$ at a constant surface pressure. This result implies that the interactions between SA and ODA molecules is most significant at $X_{SA} = 0.5$. However, the maximum deviation is only ≈3%, which is much smaller compared with that for DPPC/DHDP mixed monolayer (about 30%).[30] It is also found that the surface pressure has no significant effect on the values of A_{ex}/A_{id} which can be attributed to the small interaction of the two compounds. The small extent of the deviation of A_{ex}/A_{id} and the nearly linear relationship of Figure 2a both implied that SA and ODA molecules were nearly ideally mixed or not completely miscible. This result is consistent with that observed from the relaxation behavior of SA/ODA mixed monolayer in a previous paper.[28]

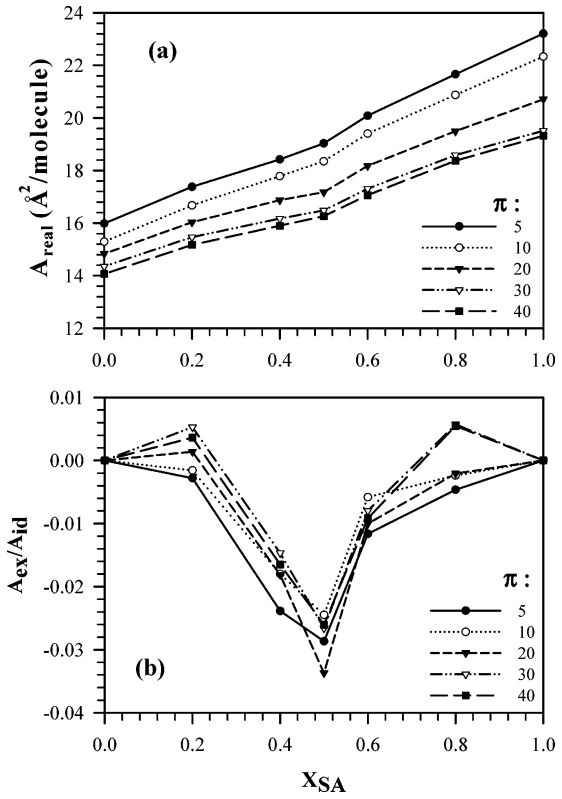

Figure 2. Area per molecule (a) and A_{ex}/A_{id} (b) as a function of composition for mixed SA/ODA monolayers on water subphase at various surface pressures.

Phases of SA/ODA Monolayers Observed by Brewster Angle Microscopy. The BAM images shown in Figure 3 exhibit the morphological information on SA monolayer at different points of the $\pi-A$ isotherm. When the occupied area of molecule is large, no light is reflected from the gas/water interface and a dark image was observed, which is identified to be the gas phase. Upon monolayer compression, bright zones of low contrast appear and the brightness and area of these zones increase gradually, indicating the increasing density of the monolayer and the formation of liquid phase. The bright zones tend to form a network structure, as shown in Figure 3a, with curve boundary between the gas and liquid phases. It is more likely that the gas phase forms elliptical domains (dark region) and disperses in the network of liquid phase. The gas/liquid coexistence phases persist before the lift-off point of isotherm. As shown in Figure 3b, the liquid phase covers nearly the entire monolayer at $\pi = 0.2$ mN/m and $A = 25.3$ Å^2/molecule, but small dark regions can also be observed across the phase boundary. Upon further compression, the gas-phase zone disappears soon, but at some where bright dots or curve lines form instead of the sharp boundary, which was attributed to the mismatch between various domains of liquid phases. Figure 3b also shows the typical morphology of stearic acid in the liquid state. The domains of various liquid phases exhibit a mosaic texture which has been reported in the literature for the

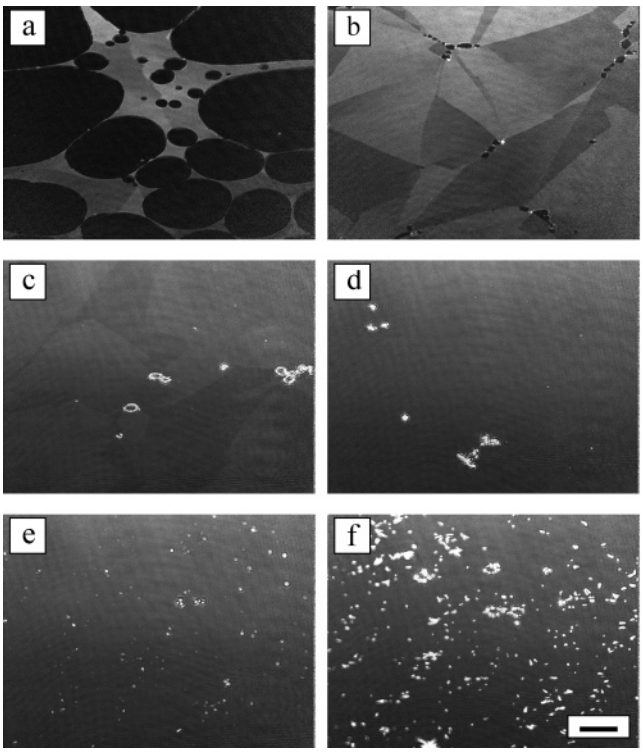

Figure 3. BAM images of pure SA monolayer on air/water interface at 25 °C. The images correspond to states of (a) $A = 28.5$ Å^2/molecule, $\pi = 0$ mN/m; (b) $A = 25.3$ Å^2/molecule, $\pi = 0.2$ mN/m; (c) $\pi = 18.4$ mN/m; (d) $\pi = 40.2$ mN/m; (e) $\pi = 44.5$ mN/m near collapse point; (f) $\pi = 25.7$ mN/m after collapse point. The length bar corresponds to a length of 50 μm.

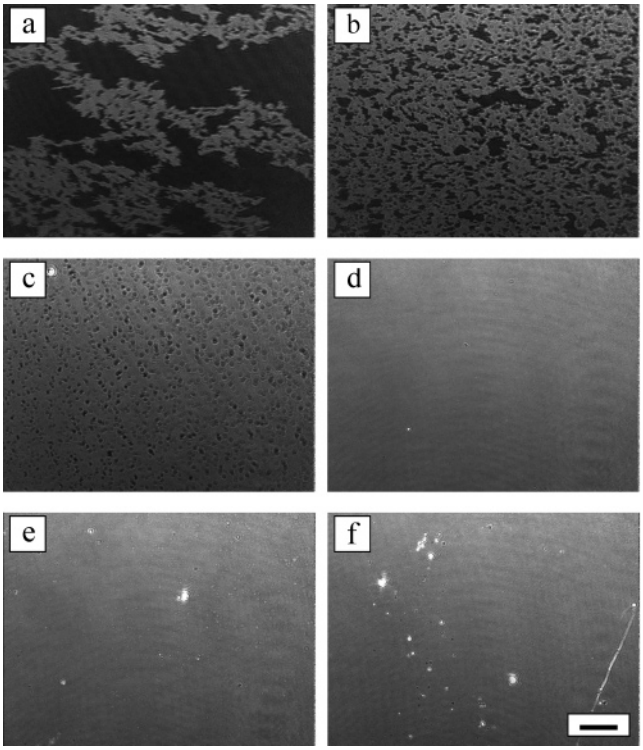

Figure 4. BAM images of pure ODA monolayer on air/water interface at 25 °C. The images correspond to states of (a) $A = 24.7$ Å^2/molecule; (b) $A = 22.5$ Å^2/molecule; (c) $A = 16.5$ Å^2/molecule, near the lift-off point; (d) $\pi = 55.2$ mN/m; (e) $\pi = 61.5$ mN/m; and (f) $\pi = 63.8$ mN/m near the collapse point. The length bar corresponds to a length of 50 μm.

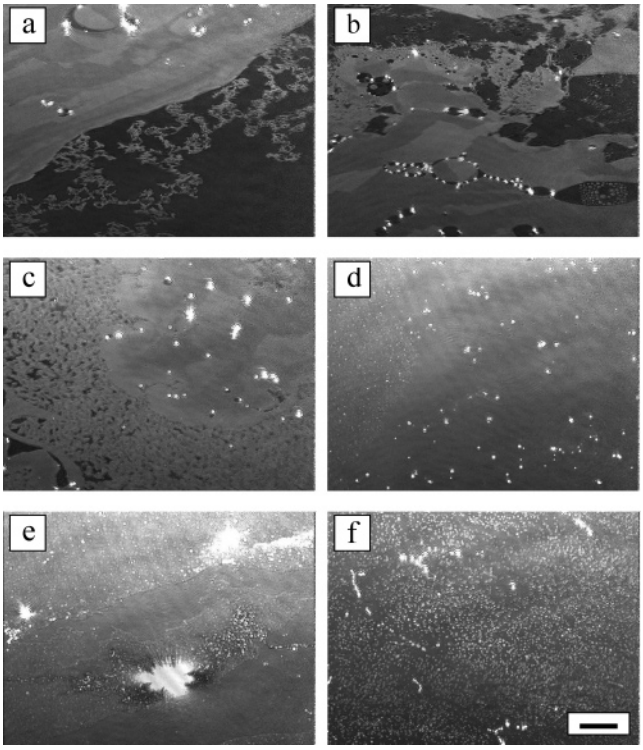

Figure 5. BAM images of SA/ODA mixed monolayer on air/water interface at 25 °C. The mole ratio of SA is 0.5, and the images correspond to the states of (a) $A = 32.9$ Å^2/molecule; (b) $A = 28.1$ Å^2/molecule; (c) $A = 22.4$ Å^2/molecule; (d) $\pi = 30.4$ mN/m; (e) $\pi = 47.2$ mN/m; near collapse point; and (f) $\pi = 34$ mN/m after collapse. The length bar corresponds to a length of 50 μm.

monolayers of fatty acid.[31,32] The contrast between the mosaic domains decreases when the surface pressure is increased further (Figure 3c), and a uniform morphology is approached after passing the phase transition pressure (27 mN/m). The uniform phase image is identified to be the solid phase of SA monolayer and persists in the following compression process up near the collapse pressure of SA (Figure 3d). However, large bright dots can occasionally be observed on the SA monolayer even when the solid phase is attained (Figure 3d). Such aggregative structure was supposed to form in the early stage of the compression process caused by the mismatch of various domains shown in Figure 3b. When the surface pressure increases near the collapse point, bright dots of high density form abruptly as demonstrated in Figure 3e, indicating the collapse of monolayers to be 3-dimensional (3D) aggregates. The aggregates grow in size and density when the surface pressure decreases after collapse, and an image is shown for $\pi = 25.7$ mN/m (Figure 3f).

The BAM morphology of ODA is essentially different from that of SA as illustrated in Figure 4. The coexisting gas and liquid phases were observed before the lift-off point of the isotherm (Figure 4a,b), which is similar to that for SA monolayer. However, the liquid phases of ODA monolayer did not show condensed patch domains as for the SA monolayer but exhibit a cloudy-like morphology with dendritic boundary. Such behavior of ODA monolayer is attributed to the higher hydrophilic property of amine group compared with carboxylic group of SA, which can be verified by the higher solubility of ODA in the water. The higher interaction between the amine group and water promotes the spreading of ODA molecules on the gas/water interface. That is, the coherent interaction among hydrophobic tails of ODA molecules is less than the interaction between amine group and water. As a consequence, the liquid phase of ODA did not form condensed domains as that of SA. Upon compression, the area of liquid phase increases and the gas phase (the dark regions) seems to disperse among the liquid phase. Near the lift-off point, the dispersed gas phase can still be observed on the matrix of liquid phase. A uniform condensed phase appears when the pressure increases near the phase transition point ($\approx$10 mN/m) and persists up about $\pi = 55.2$ mN/m (Figure 4d). At higher surface pressure, aggregates dots gradually appear with lower contrast than those found on SA monolayer (Figure 4e), and a more significant collapse phenomenon can be inspected near the collapse pressure (Figure 4f).

Mixed monolayer with 50 mol % of SA was used to demonstrate the phase images of mixed monolayers prepared by the 2D mixing and is shown in Figure 5. At high surface area, phases equivalent to SA and ODA can simultaneously be observed on the mixed monolayer as shown in the upper (SA) and lower (ODA) regions of Figure 5a. Such results sustain the previous inference that SA and ODA molecules are not well mixed in the monolayer by the 2D contact. Since SA molecules prefer to aggregate as 2D domains on the water surface, it is not easy for the two components to contact completely between each other. Upon compression, the phases of SA and ODA approach closely. In Figure 5b ($A = 28.1$ Å^2/molecule), the mosaic domains of SA can clearly be observed in the lower region, and the darker domain on the upper corner belongs to that of ODA. In addition to the two regions that can easily be identified as the pure components, an intermediate phase did exist between the two pure ones. The intermediate phase has a porous structure and is supposed to be caused from the intermixing of SA and ODA on the phase boundary. Two separated phases can always be observed in the further compression process (Figure 5c,d). The first one is mainly composed by SA with fewer bright dots dispersing in it (upper-

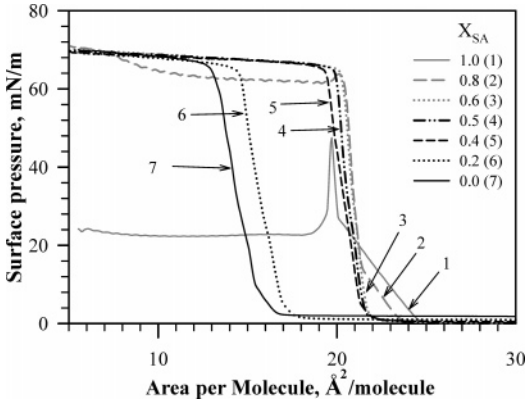

Figure 6. Surface pressure−area per molecule isotherms of mixed ODA/SA monolayers prepared by premixing the two components in chloroform first and then dispersed on the air/water interface.

right region in Figure 5c). The formation of the aggregative structure (the bright dots) on the boundary of SA mosaic domains seems to be enhanced by the presence of ODA. The second phase (on the left sides of Figure 5c,d) exhibits a more heterogeneous image and is supposed to contain both SA and ODA with SA disperses in ODA matrix. On further compression, the holes in the second phase disappear gradually, and instead, densely distributed bright dots were observed. The dense bright dots are supposed to be formed as a result of the dispersed SA in the ODA. Such aggregative dots will grow significantly to be bright domains near the first collapse point of the monolayer (Figure 5e). After collapse, the 3D structure grows rapidly on both regions and finally disperses in the entire monolayer (Figure 5f).

2. Mixed Monolayer Prepared by Premixing of SA and ODA in Spreading Solvent. The previous results infer that SA and ODA are not able to mix well by mixing on the air/liquid interface. As a comparison, the two components were mixed first in chloroform and then dispersed on the subphase. The $\pi-A$ isotherms of the mixed monolayers prepared by this method are shown in Figure 6. Apparently, the results are significantly different from those shown in Figure 1. In general, these monolayers have low compressibility as that of ODA, and nearly all the isotherms of mixed monolayers shift right compared to those of the isotherm with similar composition shown in Figure 1. Except for the monolayer with composition $X_{SA} = 0.2$, all the isotherms locate closely. In these mixed monolayers, the phase transition points of the pure monolayers are not observed, and the collapse pressures all resemble that of ODA which are also list in Table 1. All the present results indicate that the two components are completely miscible.

The mean areas per molecule of the mixed monolayers estimated from Figure 6 are shown in Figure 7a. The relation of the mean area with composition has large deviation from the linear relationship, which implies that the mixed monolayer deviates greatly from the ideal mixture. Such inference can also be sustained by the values of A_{ex}/A_{id} shown in Figure 7b. The excess surface area is predominately positive, and the value of A_{ex}/A_{id} is nearly one order larger than those shown in Figure 2b. The maximum deviation of the mixed monolayers occurs at composition of $X_{SA} = 0.4$. With increasing surface pressure, the deviation becomes larger, indicating the higher interaction between SA and ODA when the molecules were packed closely.

The BAM phase images of the mixed monolayer prepared by premixing the two compounds, as shown in Figure 8, also exhibit large difference to that prepared by 2D mixing. In the gas/liquid coexisting phase, both phases can easily be identified

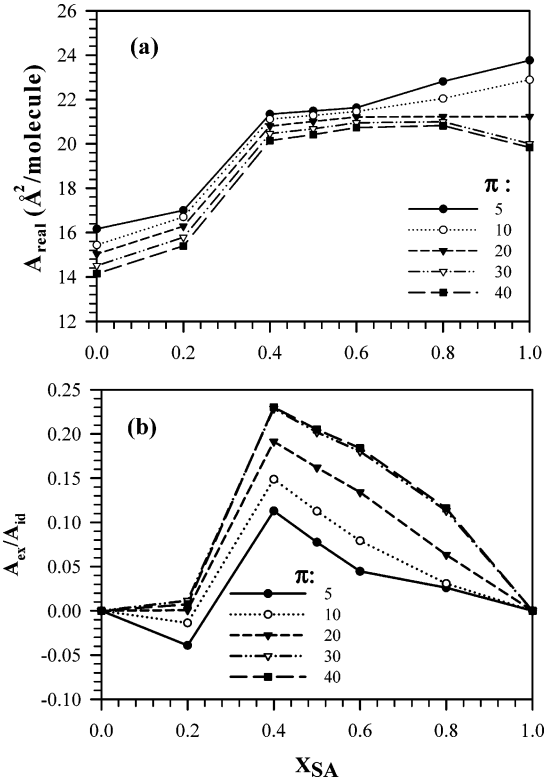

Figure 7. Area per molecule (a) and A_{ex}/A_{id} (b) as a function of composition for mixed SA/ODA monolayers prepared by premixing the two components in chloroform. These data were estimated from isotherms in Figure 6.

(Figure 8a,b). The domain of the liquid phase (the bright region) has completely different morphology as those of pure SA and ODA. Besides, when careful inspection was paid on the dark region, domains of very low contrast can be observed. Such low contrast domain represents a more dilute phase and will become more visible on further compression (Figure 8b). With decreasing surface area, a uniform liquid phase forms gradually before significant elevation of surface pressure (Figure 8c,d). After surface area decreases below the lift-off point of isotherm, the surface pressure increases steeply while the BAM morphology remains uniform without significant appearance of aggregative structure. Such results indicate that the monolayer is rigid and stable. At surface pressure near the collapse point, bright curves form on the monolayer as shown in Figure 8e. Instead of the dot or domain type of the collapse structure, as that shown on SA and ODA monolayers, the curve or strip structure becomes the main morphology of the collapse state. This structure is a character of a rigid monolayer, on which the 3D aggregates do not form by nucleation of point sites. On the other hand, the monolayer is supposed to be pushed upward and forms a folding strip upon overcompression. After collapse pressure, such folding structure grows quickly by increasing both density and size (Figure 8f).

The above results tell that uniform phase is formed for the SA/ODA mixed monolayer prepared by premixing of the two compounds in spreading solvent. Besides, special interaction exists between SA and ODA. The positive deviation of A_{ex}/A_{id} in a mixed system may imply that the interaction is repulsive and thus the mean area becomes larger. However, this inference also implies that the attractive force between homomolecules (SA to SA or ODA to ODA) is larger than the interaction between SA and ODA. In such conditions, the two components should prefer to contact with themselves rather than with heteromolecules, and thus, a well-mixed monolayer cannot be

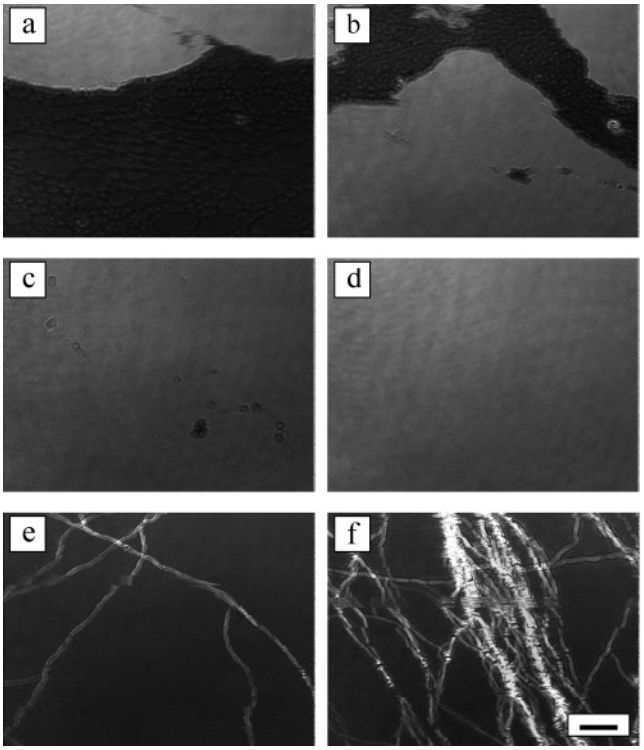

Figure 8. BAM images of SA/ODA mixed monolayer prepared by premixing the two components in chloroform and then spreading on air/water interface. The mole ratio of SA is 0.5, and the images correspond to the states of (a) $A = 31.3$ Å^2/molecule; (b) $A = 27.8$ Å^2/molecule; (c) $A = 26.4$ Å^2/molecule; (d) $A = 24.0$ Å^2/molecule; (e) $\pi = 59.6$ mN/m, near collapse; and (f) $\pi = 61.3$ mN/m, after collapse. The length bar corresponds to a length of 50 μm.

attained. This inference is contrary to the well-mixed system obtained in the present study. According to the definition, a higher surface pressure represents a lower surface tension decreased by the existing of monolayer. In Figure 6, the isotherm of mixed monolayer lifts at a larger area compared to that of an ideal mixture, which also means that the surface tension is decreased by a lower concentration of molecules on the air/liquid interface. That is, the molecules in the mixed monolayer have higher surface activity than that of the pure components. This result can be attributed to the synergistic effect of the mixed system.

Because SA and ODA are belong to acid and base, respectively. It is possible that the two components react to be salt.[24] It is also possible that the two headgroups are ionized and adsorb together to form a structure similar to that of "catanionic surfactant".[33,34] No mater what is formed, they all have a molecular structure with a large polar group and two alkyl chains. Monolayers composed by such molecules were found to have a condensed and rigid structure, especially for the SA and ODA which have long carbon chains.

Conclusion

The present results show that the mixing and the miscibility of SA and ODA in the mixed monolayer are affected by the spreading methods used in preparing the monolayer. When SA and ODA are spread individually onto the subphase, the two compounds cannot get well mix via 2-D contact and phase separation exists. As a result, individual characteristics of SA and ODA still preserve in the mixed monolayers as inspected from the $\pi-A$ curves, collapse pressures, and the BAM images. On the contrary, when SA and ODA are premixed in the spreading solvent before spreading on the subphase, a well-mixed phase is formed for the monolayer. The isotherms of mixed monolayers exhibit low compressibility, high collapse pressure, and highly rigid characteristic. The mean molecular area is deviated largely from that of an ideal mixture and a positive deviation is found. The higher interaction between SA and ODA molecules in the mixed monolayer is attributed to the possible formation of "catanionic surfactant" or to the acid−base reaction.

References and Notes

(1) Tieke, B.; Fulda, K.-U.; Kampes, A. In *Nano-Surface Chemistry*; Rosoff, M., Ed.; Mono- and Multilayers of Spherical Polymer Particles Prepared by Langmuir−Blodgett and Self-Assembly Techniques; Marcel Dekker: New York, 2002; Chapter 5, p 213.

(2) Schwartz, D. K. *Surf. Sci. Rep.* **1997**, *27*, 241.

(3) Roberts, G., Ed.; *Langmuir−Blodgett Films*; Plenum Press: New York, 1990.

(4) Ariga, K.; Shin, J. S.; Kunitake, T. *J. Colloid Interface Sci.* **1995**, *170*, 440−448.

(5) Brinks, B. P. *Adv. Colloid Interface Sci.* **1991**, *34*, 343.

(6) Morelis, R. M.; Girard-Egrot, A. P.; Coulet, P. R. *Langmuir* **1993**, *9*, 3101−3106.

(7) Stine, K. J.; Moore, B. G. In *Nano-Surface Chemistry*; Rosoff, M., Ed.; Langmuir Monolayer: Fundamental and Relevance to Nanotechnology; Marcel Dekker: New York, 2002; Chapter 3, p 59.

(8) Muramatsu, K.; Takahashi, M.; Tajima, K.; Kobayashi, K. *J. Colloid Interface Sci.* **2001**, *242*, 127.

(9) Du, H.; Bai, Y. B.; Hui, Z.; Li, L. S.; Chen, Y. M.; Tang, X. Y.; Li, T. J. *Langmuir* **1997**, *13*, 2538.

(10) Vollhardt, D.; Retter, U. *Langmuir* **1998**, *14*, 7250.

(11) Angelova, A.; Vollhardt, D.; Ionov, R. *J. Phys. Chem.* **1996**, *100*, 10710.

(12) Vollhardt, D.; Retter, U.; Siegel, S. *Thin Solid Films* **1991**, *199*, 189.

(13) Vollhardt, D.; Gutberlet, T. *Colloids Surf. A: Physicochem. Eng. Aspects* **1995**, *102*, 257.

(14) Lee, Y. L. *Langmuir* **1999**, *15*, 1796.

(15) Ganguly, P.; Paranjape, D. V.; Rondelez, F. *Langmuir* **1997**, *13*, 5433.

(16) Chovelon, J. M.; wan, K.; Jaffrezic-Renault, N. *Langmuir* **2000**, *16*, 6223.

(17) Flores, A.; Ize, P.; Ramos, S.; Castillo, R. *J. Chem. Phys.* **2003**, *119*, 5644.

(18) Ras, R. H. A.; Johnston, C. T.; Franses, E. I.; Ramaekers, R.; Maes, G.; Foubert, P.; De Schryver, F. C.; Schoonheydt, R. A. *Langmuir* **2003**, *19*, 4295.

(19) Mayya, K. S.; Patil, V.; Sastry, M. *Langmuir* **1997**, *13*, 2575.

(20) Ganguly, P.; Paranjape, D. V.; Sastry, M. *Langmuir* **1993**, *9*, 571.

(21) Ganguly, P.; Paranjape, D. V.; Sastry, M. *J. Am. Chem. Soc.* **1993**, *17*, 793.

(22) Chou, T. H.; Chang, C. H. *Colloids Surf. B* **2000**, *17*, 71.

(23) Gabrielli, G.; Puggelli, M.; Gilardoni, A. *Prog. Colloid Polym. Sci.* **1992**, *89*, 227.

(24) Puggelli, M.; Gabrielli, G.; Caminati, G. *Thin Solid Films* **1994**, *244*, 1050.

(25) Ku, I.-H.; Lee, Y.-L.; Chang, C.-H.; Yang, Y.-M.; Maa, J.-R. *Colloids Surf. A* **2001**, *191*, 223.

(26) Sheu, C.-W.; Chang, C.-H.; Lee, Y.-L.; Yang, Y.-M.; Maa, J.-R. *J. Chin. Inst. Chem. Eng.* **2002**, *33*, 573.

(27) Emelianov, I. L.; Khatko, V. V. *Sens. Actuators B* **1999**, *60*, 221.

(28) Lee, Y.-L.; Liu, K.-L. *Langmuir* **2004**, *20*, 3180.

(29) Ye, S.; Noda, H.; Nishida, T.; Morita, S.; Osawa, M. *Langmuir* **2004**, *20*, 357.

(30) Chou, T.-H.; Chang, C.-H. *Langmuir* **2000**, *16*, 3385.

(31) Overbeck, G. A.; Mobius, D. *J. Phys. Chem.* **1993**, *97*, 7999−8004.

(32) Riviere, S.; Henon, S.; Meunier, J.; Schwartz, D. K.; Taso, M.-W.; Knobler, C. M. *J. Chem. Phys.* **1994**, *101*, 10045.

(33) Viseu, M. I.; Goncalves da Silva, A. M.; Costa, S. M. B. *Langmuir* **2001**, *17*, 1529−1537.

(34) Goncalves da Silva, A. M.; Viseu, M. I.; Campos, C. S. C.; Rechena, T. *Thin Solid Films* **1998**, *320*, 236−240.